In vitro and In vivo Investigation of poly(lactic acid)/hydroxyapatite nanoparticle scaffold containing nandrolone decanoate for the regeneration of critical-sized bone defects

Majid Salehi [1, 2], Arman Ai [3], Arian Ehterami [4], Masoumeh Einabadi [5], Alireza Taslimi [6], Armin Ai [6],*
Hamta Akbarzadeh [6], Ghazal Jabal Ameli [6], Saeed Farzamfar [7], Sadegh Shirian [8], Nahal Azimi [6], Faezeh
Sadeghi [6], Naghmeh Bahrami [9, 10], Arash goodarzi [11], Jafar Ai [7]

[1] *Department of Tissue Engineering, School of Medicine, Shahroud University of Medical Sciences, Shahroud, Iran*
[2] *Tissue Engineering and Stem Cells Research Center, Shahroud University of Medical Sciences, Shahroud, Iran*
[3] *School of Medicine, Tehran University of Medical Sciences, Tehran, Iran*
[4] *Department of Mechanical and Aerospace Engineering, Islamic Azad University, Science and Research Branch, Tehran, Iran*
[5] *Department of Biology, Islamic Azad University, Jahrom Branch, Jahrom, Iran*
[6] *Dentistry Student, Scientific Research Center, School of Dentistry, Tehran University of Medical Sciences, Tehran, Iran*
[7] *Department of Tissue Engineering and Applied Cell Sciences, School of Advanced Technologies in Medicine, Tehran University of Medical Sciences, Tehran 1417755469, Iran*
[8] *Department of Pathology, School of Veterinary Medicine, Shahrekord University, Shahrekord, Iran*
[9] *Craniomaxillofacial Research Center, Tehran University of Medical Sciences, Tehran, Iran*
[10] *Department of Oral and Maxillofacial Surgery, School of Dentistry, Tehran University of Medical Sciences, Tehran, Iran*
[11] *Department of Tissue Engineering, School of Advanced Technologies in Medicine, Fasa University of Medical Sciences, Fasa, Iran*

ABSTRACT

Objective(s): Bone tissue engineering is aimed at the fabrication of bone graft to ameliorate bone defects without using autografts or allografts.
Materials and Methods: In the present study, the coprecipitation method was used to prepare hydroxyapatite (HA) nanoparticles containing nandrolone. To do so, 12.5, 25, and 50 mg of nandrolone were loaded into poly(lactic acid) (PLA)/nano-HA, and the freeze casting method was used to fabricate porous scaffolds. The morphology, mechanical strength, wettability, porosity, degradation, blood compatibility, and cellular response of the scaffolds were evaluated using various tests. For further investigation, the developed scaffolds were incorporated into the rat calvaria defect model, and their effects on bone healing were evaluated.
Results: The obtained results indicated that the fabricated scaffolds had the approximate porosity of 80% and compress strength of 6.5 MPa. Moreover, the prepared scaffolds had appropriate hydrophilicity, weight loss, and blood compatibility. Furthermore, the histopathological findings demonstrated that the defects filled with the PLA/nano-HA scaffolds containing 25 mg nandrolone healed better compared to the other study groups.
Conclusion: Therefore, it was concluded that the scaffolds containing nandrolone could be used in bone regeneration.

Keywords: *Bone Healing, Freeze Casting Method, Hydroxyapatite, Nandrolone, Scaffold*

* Corresponding Author Email: arminai@gmail.com

INTRODUCTION

Bone defects affect numerous individuals per year and are mainly caused by age-related conditions, diseases or trauma. Due to the complications (e.g., immune rejection) and increased limitation in allograft and autograft resources, various alternative methods in tissue engineering have been applied to replace the failing or malfunctioning tissues using the combination of scaffolds, appropriate cells, and signaling molecules [1, 2]. Previous studies have used various techniques to fabricate bone scaffolds, while some methods have been applied more commonly in this regard, such as freeze casting [3], electrospinning [4], and foam casting[5]. Freeze casting is a practical method that is widely used to fabricate unidirectional porous polymeric or/and ceramic structures. In this technique, a liquid suspension freezes rapidly in an isolated mold using liquid nitrogen, followed by the sublimation of the frozen liquid suspension phase in vacuum conditions in order to produce an anisotropic porous microstructure. The production of lamellar structures is also possible in this method by controlling the growth direction of the ice crystals [6]. Poly (lactic acid) (PLA) is biodegradable aliphatic polyester, which has recently attracted the attention of researchers due to the fact that it could be derived from renewable resources, such as corn and sugar beets. On the other hand, PLA has low mechanical strength[7], and the addition of a small amount of layered silicate particles with high aspect ratio could enhance the mechanical and physical properties, thereby resulting in higher strength, stiffness, heat resistance, and UV resistance, while maintaining the transparency and impact properties [8, 9].Calcium hydroxyapatite (HA) is a mineral component inside the bones and teeth of humans, with the chemical formula of Ca(2)6Ca(1)4(PO4)6(OH)2 (P63/m) [10]. With its appropriate biocompatibility and sufficient biodegradation rate, HA is not only used in orthopedics as a bone graft, but it also is applied in drug delivery systems for controlled release [11-13]. Moreover, HA has a proper structure for the incorporation of various ionic substitutions [14].

Nandrolone (ND) is a class-II anabolic androgenic steroid (AAS), consisting of 19 nortestosterone derivatives [15]. In general, AAS is a wide and rapid-growing group of synthetic androgens, which are used clinically and illicitly. ND is also widely used in clinical practice, surgery, radiation therapy, burn wound healing, and treatment of traumas and various forms of anemia [16]. Owing to its remarkable properties (e.g., tissue-building improvement, maintenance of strength, muscle mass, and libido) ND is commonly used by athletes to improve strength, accelerate muscle development, promote recovery, and improve aggression [17]. In addition, this compound is prescribed for adolescents due to its anabolic and muscle-building properties [18-21]. It is also notable that ND is considered to be the most generally abused AAS across the world [15, 22, 23]. to date, few studies have assessed the role of ND decanoate in bone defect healing despite its established positive effects on bone quality and muscular tropism [24, 25]. In the present study, PLA scaffolds containing nano-HA and ND fabricated via the freeze casting method were used for the local administration and evaluation of the bone healing activity in bone tissue engineering. Furthermore, the properties of the PLA scaffolds containing nano-HA/ND were investigated using various *in-vitro* methods, and the *in-vivo* bone healing efficacy of the scaffolds was also evaluated in the rat calvaria defect model.

MATERIALS AND METHODS
Applied chemicals

In this study, the materials and solvents were purchased from Sigma-Aldrich (St. Louis, USA) and Merck (Darmstadt, Germany), respectively unless otherwise noted.

Experimental Methods
Preparation of the HA Nanoparticles

The HA nanoparticles (nano-HA) were synthesized in accordance with the protocol described by Salehi et al. [26]. In brief, 7.48 grams of Ca $(OH)_2$ was dissolved in 100 milliliters of an ethanol-water mixture (1:1 v/v) at the temperature of 33 and stirred for three hours. During 24 hours, 6.7 grams of $NH_4H_2PO_4$ in 100 milliliters of water was added to the $Ca(OH)_2$ solution, and the pH of the prepared slurry was adjusted to 11 by adding NaOH (1 M). Finally, the slurry was frozen at the temperature of -80°C for 24 hours and freeze-dried (Telstar, Terrassa, Spain) for 48 hours. The mean diameters of the nano-HA were calculated after three runs using a dynamic light scattering (DLS) device (model: K-One; Seoul, South Korea).

Fabrication of the PLA/Nano-HA Scaffold

Using the Freeze Casting Technique Initially, the polymer solution was prepared by adding the PLA pellets (10 wt% for the solution) and nano-HA [27] to 1,4-dioxane and stirred at the temperature of 30°C for 24 hours at the agitation rate of 500 rpm and sonication at room temperature for four hours. Afterwards, the ND decanoate was added to the prepared solution with the weight of 12.5, 25, and 50 milligrams per 1,000 milligrams of PLA. Following that, the solution was transferred into the freeze casting device, frozen at the temperature of -196°C for six hours, and freeze-dried (Telstar, Terrassa, Spain) for 72 hours. The ready-to-use scaffolds were preserved in vacuumed packs until the surgical procedure.

Characterization of the Nano-HA and scaffolds

The particle size and zeta potential of the nanoparticles was measured using the Zetasizer device (model: Nano-ZS; Malvern Instruments, Worcestershire, United Kingdom). The analysis was performed 22 times at the temperature of 25°C using the samples diluted in distilled water with the viscosity of 0.8872 cP.

At the next stage, the samples were coated by gold for 250 seconds using a sputter coater (Quorum Technologies, Sussex, United Kingdom) at the accelerating voltage of 20 kV. Following that, a scanning electron microscope (SEM; Crossbeam®, 1540XB by Zeiss) was used to evaluate the 3D structure and morphology of the scaffolds. In addition, the pore size was measured in a minimum of 10 pores in the fabricated scaffolds.

The compressive strength and modulus of the scaffold were examine using the mechanical testing machine (Santam, IRI) at the crosshead speed of 1 mm/min with the load cell of 1,000N. The samples were cylinders of approximately 10 mm in diameter and 20 mm in height. The wettability of the produced scaffolds was also determined using the static contact angle measuring device (KRUSS, Hamburg, Germany). The mean water contact angle value was evaluated using deionized water on the three sections of each scaffold.

The liquid displacement method was used to evaluate the porosity of the scaffolds (Equation 1) [28].

$$Porosity\ (\%) = \frac{V1-V3}{V2-V3} \times 100 \quad (1)$$

In Equation 1, $V1$ is the initial volume of absolute ethanol, $V2$ represents its volume after scaffold immersion (ethanol filling the pores), and $V3$ shows the residual volume of ethanol after the scaffold removal. Each scaffold was analyzed in triplicate. To evaluate the biodegradability of the scaffolds, their weight loss was monitored for 60 days. In brief, the samples were soaked in 10 milliliters of simulated body fluid (SBF) at the temperature of 37°C, and Equation 2 was used to calculate the weight loss, as follows:

$$Weight\text{-}loss\ (\%) = \frac{W1-W2}{W1} \times 100 \quad (2)$$

where $W1$ denotes the original weight of the sample, and $W2$ is the dry weight of the sample after removal from SBF [3]. In addition, the mean value of the three samples for each scaffold was reported. In this research, a hemolysis assay (ISO 10993-4) was used to examine the blood biocompatibility of the produced scaffolds. To this end, two milliliters of fresh anti-coagulated human blood, which was collected from healthy volunteers, was diluted with 2.5 milliliters of normal saline. Following that, the samples were immersed in diluted blood (0.2 ml), and the mixture was incubated at the temperature of 37°C for 60 minutes and centrifuged for 10 minutes at 1,500 rpm. The supernatant was transferred to a 96-well plate, in which the optical density (OD) was measured at 545 nanometers using the BioTek Synergy 2 Multimode Microplate Reader. The mean values obtained from the three measurements were calculated. It is notable that the positive control samples contained 0.2 milliliter of diluted blood in 10 milliliters of deionized water, and the negative control samples contained 0.2 milliliter of diluted blood in 10 milliliters of normal saline. Moreover, the hemolysis degree was calculated using Equation 3, as follows:

$$Hemolysis\ assay\ (\%) = \frac{Dt-Dnc}{Dpc-Dnc} \times 100 \quad (3)$$

where Dt indicates the OD of test samples, Dnc is the OD of the negative controls, and Dpc denotes the OD of the positive controls.

Cell culture assessment

At this stage, bone marrow-derived mesenchymal stem cells (BMSCs) were cultured in Dulbecco's modified Eagle's medium (DMEM-Gibco-BRL, Life Technologies, Grand Island, NY), supplemented with 10% fetal bovine serum and antibiotics (100 unit/ml penicillin G and 100 µg/ml streptomycin; Gibco-BRL, Life Technologies) and incubated with 5% CO_2 at the temperature of 37°C. The media was changed every 24 hours.

For cell seeding, the scaffolds were placed in a 96-well plate and sterilized via ultraviolet light irradiation (254 nm) on both sides for 30 minutes

Nanomed. J. 7(2): 115-123, Spring 2020

117

each in a laminar flow hood and seeded with 1×10^4 cells. The proliferation of the cells on the scaffolds was assessed using the 3-(4, 5-dimethylthiazol-2-yl)-2, 5-diphenyltetrazolium bromide (MTT) assay kits (Sigma-Aldrich, St. Louis, USA) in accordance with the instructions of the manufacturer. In this process, the cells in the wells of the plate without scaffolds were considered as controls. All the experiments were performed in triplicate, and the OD was measured using a microplate reader (Thermo Scientific, USA).

Animal and surgical procedures

This stage of the study was performed on 24 adult male Wistar rats (weight: 250-300 g). The animals were kept in sole cages and fed *ad libitum*. The study protocol was reviewed and approved by the Ethics Committee of Shahroud University of Medical Sciences in terms of the use of experimental animals in scientific procedures.

The surgical procedures were performed in sterile conditions in a veterinary operation room. General anesthesia was induced via the intraperitoneal injection of ketamine hydrochloride (100 mg/kg) and xylazine (10 mg/kg), and the areas of the scalp covering the calvarial vault were shaved and prepped with povidone iodine. After the infiltration of local anesthesia (2% lidocaine with 1:100,000 epinephrine), an incision was made along the midline. Full-thickness skin and the periosteum were reflected to expose the cranium surface. In addition, an electrical bone trephine bur (Strong Co., Seoul, South Korea) was employed to create one circular defect (diameter: 7 mm, depth: 2 mm) around the sagittal suture with normal saline irrigation. During drilling, excellent care was provided to protect the dura mater against damage. The bone defects were either left empty or treated with PLA/n-HA or PLA/nano-HA with variable levels of ND in the defected areas. At the end of the surgery, the defect sites were sutured, and meloxicam (1 mg/kg) and enrofloxacin (10 mg/kg) were injected to each animal for five days. Eight weeks after the surgery, the animals were euthanized through the intravenous injection of ketamine hydrochloride (50 mg/kg) and xylazine hydrochloride (5 mg/kg), and gallamine triethiodide (1 mg/kg; Specia, Paris, France) was injected intracardially in order to stop the breathing of the anesthetized animals.

Histopathological analysis

Bone tissues were harvested eight weeks postoperatively, initially removed from the muscles and soft tissues, fixed in 10% neutral buffered formalin solution for 48 hours, and decalcified with 14% EDTA (pH: 7.4) for 28 days. At the next stage, the decalcified bone samples were dehydrated in a gradient series of ethanol, cleared in xylene, and embedded in paraffin. The sections (thickness: 5 μm) were prepared and stained with hematoxylin and eosin (H&E) and Masson's trichrome (MT). The histological sections were evaluated using a light microscope (model: Olympus BX51; Olympus, Tokyo, Japan).

Statistical analysis

The quantitative data were analyzed using one-way analysis of variance (ANOVA) and Tukey's post-hoc test. In case of significant differences ($P<0.05$), data analysis was performed using Mann-Whitney U test. All the statistical analyses were carried out in GraphPad Prism software version 6.00 (Graphpad Prism, Inc., San Diego, CA).

RESULTS
Characterization of the HA Nanoparticles

According to the results of DLS analysis, the mean diameter of the HA nanoparticles was 397.5±21.32 nanometers, and their polydispersity index was estimated at 0.28. Moreover, the zeta potential measurement indicated that the nano-HA and nano-HA-ND nanoparticles had the mean surface charge of +4.03±0.62 and +17.89±0.74 mV, respectively.

Characterization of the fabricated scaffolds

As was observed in the SEM images (Fig 1-A), the PLA/HA-ND had the same morphology with irregular-shaped pores. The mean pore size in various samples was estimated at 260±12 micrometers, and the minimum required pore size for the bone tissue engineering scaffolds was determined to be approximately 100 micrometers [29]. Therefore, all the produced scaffolds could meet the minimum required pore size and were considered suitable for bone tissue engineering.

The mechanical properties of the scaffolds are presented in Table 1. According to the findings, the mean compress strength of PLA/HA was 6.03±1.15 MPa, and with the addition of ND, the strength increased to 6.93±1.04 MPa; however, the difference was not considered significant.

Hydrophilicity is considered to be an important attribute of scaffolds in cell attachments to increase bone healing [30].

Table 1. Characterization of Fabricated Scaffold

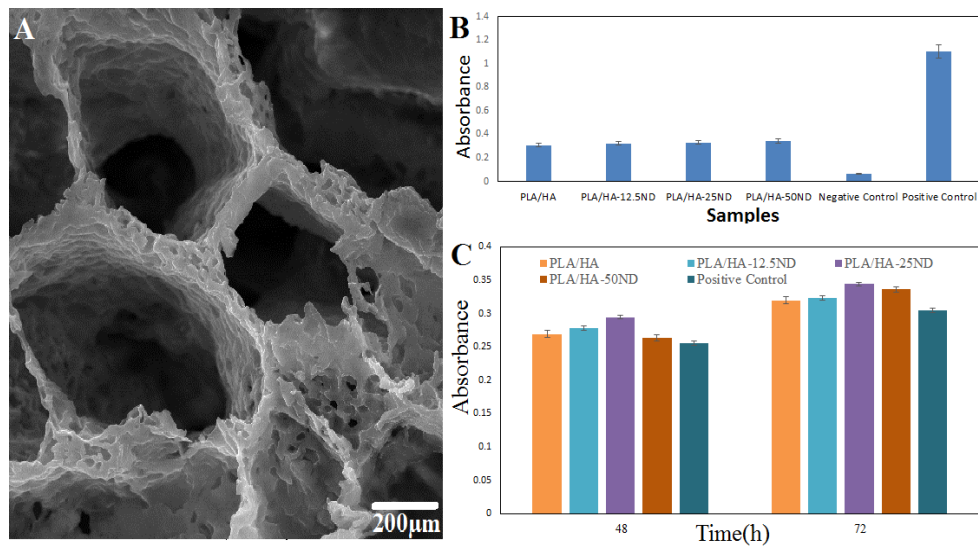| Samples	Compress strength (MPa)	Contact angle (°)	Porosity (%)	Weight-loss after 30 days (%)	Weight-loss after 60 days (%)
PLA/HA	6.03 ± 1.15	72.2 ± 1.44	86.5 ± 2.11	24.8 ± 0.26	40.9 ± 1.38
PLA/HA-12.5ND	6.48 ±0.67	75.3 ± 0.26	82.49 ± 2.48	23.47 ± 1.59	36.16 ± 1.83
PLA/HA-25ND	6. 61 ± 0.35	77.7 ± 0.51	81.23 ± 3.05	22.3 ± 2.11	33.5 ± 1.66
PLA/HA-50ND	6.93±1.04	82.3 ± 1.23	77.62 ± 2.32	20.38 ± 2.64	28.37 ± 1.25

Fig 1. A) SEM Images of PLA/HA-ND, B) Results of Hemolytic Rate Experiment, C) In-vitro Cell Culture Results (Histogram comparing proliferation of bone marrow cells on scaffolds 24 and 72 hours after cell seeding)

In this study, the water contact angles of the PLA/HA was 72.2±1.44° (Table 1). As ND is a hydrophobic material, its addition to the scaffold increase the contact angle, while the difference observed between the contact angles of the fabricated scaffolds was not considered statistically significant.

Interconnected pore and high porosity structures are considered appropriate for cell proliferation and migration, vascularization, and new bone formation all over the 3D scaffold [31]. According to the porosity measurement in this research, the addition of ND decreased the porosity, while the difference was not considered significant (Table 1).

Tissue engineering scaffolds must be selected from degradable materials in order to gradually degrade *in-vivo* and become replaced by natural extracellular matrix (ECM) [32]. Therefore, the fabricated scaffolds were characterized in terms of *in-vitro* degradation in phosphate buffered saline for 30 and 60 days (Table 1).

According to the obtained results, the addition of ND was associated with the reduced weight loss rate. In this study, the hemolysis measurements indicated the release of hemoglobin into the plasma based on erythrocyte damage, which indicated the blood compatibility of the assessed materials. The results of the hemolytic rate experiment are depicted in Fig 1-B. accordingly, the hemolysis rate of all the samples was significantly lower compared to the positive controls, and the hemolysis rate was observed to increase with the addition of ND to the PLA/HA; however, the difference in this regard was not considered significant.

Nanomed. J. 7(2): 115-123, Spring 2020

119

Cell culture assessment

The MTT assay was applied to determine the effects of the scaffolds on the proliferation and viability of the bone marrow cells. According to the findings, the addition of ND to the scaffolds resulted in the increased proliferation and viability of the bone marrow cells.

Moreover, the PLA/HA-25ND scaffolds showed higher absorbance in the MTT assay compared to the other groups (Fig 1-C).

Histopathological findings

The histological analysis of the calvaria defects in the experimental groups was performed eight weeks post-injury (Fig 2), and the rate of new bone formation was observed to be higher in the defect sites treated with PLA/HA-25ND (Fig 2-C) compared to the untreated defects and the groups receiving treatment with PLA/HA, PLA/HA-12.5 ND, and PLA/HA-50 ND. In addition, the bone gap in the untreated group (Fig 2-A) was filled by a loose areolar connective tissue, which consisted of fibrous connective tissues (green arrow) in the defected area at eight weeks postoperatively.

After eight weeks, the histopathological assessment indicated that the calvaria defects treated by PLA/HA were filled with various tissue types, such as fibrocartilage and cartilaginous tissues (Fig 2-B).

DISCUSSION

In the present study, a PLA/n-HA scaffold was fabricated and characterized for bone tissue engineering. In order to enhance the bone healing effects of the scaffold, various concentrations of ND were loaded into the scaffold, and its role in bone healing was determined based on *in-vivo* and *in-vitro* tests.

Use of biomaterials for drug delivery has enabled significant progress toward consistent bone regeneration in defect sites[33]. Pure PLA and pure HA scaffolds have been commonly used in tissue engineering [34-36].PLA is a biodegradable material with proper biocompatibility, which is widely applied in tissue engineering [37]. In some studies, PLA has been incorporated for the improvement of the mechanical properties of scaffolds [38]. On the other hand, HA is the major constituent of natural bones, and HA nanoparticles have been successfully embedded in the collagen matrix [39].Use of HA nanoparticles not only mimics the natural ECM, but it also is common in bone tissue engineering due to its bioactivity and osteoconductivity [40, 41]. The freeze casting method is considered to be an optimal process for the preparation of PLA/n-HA scaffolds since it could accommodate the incorporation of materials, producing highly porous, thin-walled architecture [6, 28].
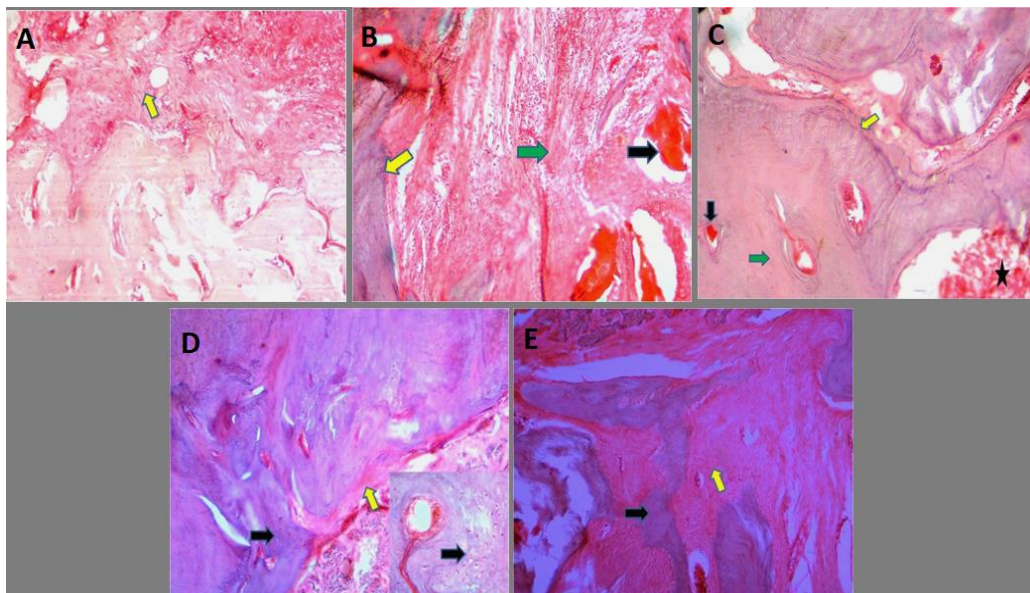

Fig 2. Histopathological Findings on Implanted Materials in Experimental Calvaria Defect; A) PLA/HA (yellow arrow: extensive fibrous connective tissue), B) PLA/HA-12.5ND (green arrow: extensive fibrous connective tissue, yellow arrow: cartilage, black arrow: fibrocartilage tissue and residual scaffold), C) PLA/HA-25ND (black arrow: residual scaffold, green arrow: woven bone, yellow arrow: fibrocartilage tissue, star: bone marrow), D) PLA/HA-25ND (black arrows: extensive cartilage tissue, yellow arrow: fibrous tissues), E) Negative Control (yellow arrow: extensive fibrocartilage tissue with superiority fibrous, black arrows: extensive cartilage tissue)

120

Nanomed. J. 7(2): 115-123, Spring 2020

The proper mechanical properties of PLA/n-HA scaffold render it an effective material to be used for drug delivery. Pore size and porosity of scaffolds have been reported to influence bone formation in *in-vitro* and *in-vivo* studies [42]. In *in-vitro* studies, low porosity has been shown to increase cell proliferation by forcing cell aggregation and stimulating osteogenesis [43]. In contrast, *in-vivo* studies have demonstrated that high porosity and pore size could increase bone growth [44]. Therefore, the porosity rate and pore size of scaffolds should be balanced to enhance bone healing. According to the literature, the minimum pore size is approximately 100 micrometers based on the cell size, migration requirements, and transport. Pore sizes near 400 micrometers are also recommended owing to the enhanced new bone formation and formation of capillaries [42].

In the current research, an *in-vitro* degradation test was carried out in SBF in order to evaluate the characteristics and degradation rate of the fabricated scaffold, and several time intervals were set to obtain the kinetic measurements. According to the obtained results, all the scaffolds lost weight during at the determined time intervals. It is also notable that the degradation rate of the scaffold increased with the addition of n-HA, which could be due to the high degradation rate of HA [45].

According to the results of the present study, the differences observed between the study group after 24 and 72 hours in the MTT assay were not statistically significant. According to the previous studies in this regard, this findings could be due to cell contact inhibition as cells discontinue proliferation after reaching confluence [46, 47]. As BMSCs have a high proliferation rate, it seems that the cells reached confluence after 24 hours, and the differences between the study groups after 72 hours were not considered significant. However, PLA/HA-25ND was observed to have higher absorbance compared to the other groups.

Previous studies have confirmed the positive effect of anti-catabolic and anabolic drugs on fracture healing in osteoporotic bone models [48]. Despite the existence and use of ND decanoate for the treatment of intact bone and muscular deteriorations, no prior studies have specifically investigated its effects on bone healing. In this regard, the findings of Demling indicated that anabolic steroids are capable of releasing the beta growth factors that stimulate bone formation

[49]. Another research also assessed the effects of ND decanoate on fracture healing [50], and ND decanoate was reported to enhance bone healing through callus formation (secondary healing) without the interference of fracture misalignment, which might complicate the interpretation of the obtained results [51, 52].

The histopathological findings of the current research are consistent with the results of the previous studies in this regard, indicating the positive effects of ND on bone healing. In the present study, the group treated with PLA/HA-25ND showed significantly enhanced bone regeneration compared to the other groups. Similarly, Pansieri et al. stated that high doses of anabolic steroids (e.g., ND decanoate) adversely affected the bone regeneration process in rats with fibular fractures and bone loss since the regeneration process did not occur in the treated animals. Furthermore, the resorption process increased on the ends of the fractured stumps [53]. This is in line with the results of the present study as the PLA/HA-50ND group had lower bone healing compared to the PLA/HA-25ND group.

CONCLUSION

In this study, PLA/n-HA/ND scaffolds were fabricated and examined for bone tissue engineering applications. According to the results, the PLA/n-HA scaffold containing 25 milligrams of ND exhibited the highest cell proliferation and viability in the bone marrow. The results of *in vivo* examinations also supported the positive effects of the ND-loaded scaffold on bone healing compared to the ND-free scaffold. Therefore, our findings provide evidence on the possible applicability of ND-containing scaffolds for the treatment of bone defects.

REFERENCES

1. Guo B, Glavas L, Albertsson A-C. Biodegradable and electrically conducting polymers for biomedical applications. Prog Polym Sci. 2013; 38(9): 1263-1286.
2. Nabavi MH, Salehi M, Ehterami A, Bastami F, Semyari H, Tehranchi M, Nabavi MA, Semyari H. A collagen-based hydrogel containing tacrolimus for bone tissue engineering. Drug Deliv Transl Res. 2019: 1-14.
3. Semyari H, Salehi M, Taleghani F, Ehterami A, Bastami F, Jalayer T, Semyari H, Hamed Nabavi M, Semyari H. Fabrication and characterization of collagen–hydroxyapatite-based composite scaffolds containing doxycycline via freeze-casting method for bone tissue engineering. J Biomater Appl. 2018; 33(4): 501-513.
4. Salehi M, Bastami F. Characterization of wet-electrospun poly (ε-caprolactone)/poly (L-lactic) acid with calcium

phosphates coated with chitosan for bone engineering. RRR 2016;1(2):69-74.

5. Ehterami A, Kazemi M, Nazari B, Saraeian P, Azami M. Fabrication and characterization of highly porous barium titanate based scaffold coated by Gel/HA nanocomposite with high piezoelectric coefficient for bone tissue engineering applications. J Mech Behav Biomed Mater. 2018; 79: 195-202.

6. Deville S, Saiz E, Tomsia AP. Freeze casting of hydroxyapatite scaffolds for bone tissue engineering. Biomater. 2006; 27(32): 5480-5489.

7. Farzamfar S, Naseri-Nosar M, Sahrapeyma H, Ehterami A, Goodarzi A, Rahmati M, Ahmadi Lakalayeh G, Ghorbani S, Vaez A, Salehi M. Tetracycline hydrochloride-containing poly (ε-caprolactone)/poly lactic acid scaffold for bone tissue engineering application: in vitro and in vivo study. Int J Polym Mater. 2019; 68(8): 472-479.

8. Alexandre M, Beyer G, Henrist C, Cloots R, Rulmont A, Jérôme R, Dubois P. "One-Pot" Preparation of Polymer/ Clay Nanocomposites Starting from Na+ Montmorillonite. 1. Melt Intercalation of Ethylene– Vinyl Acetate Copolymer. Chem Mater. 2001; 13(11): 3830-3832.

9. Lee JH, Park TG, Park HS, Lee DS, Lee YK, Yoon SC, Nam J-D. Thermal and mechanical characteristics of poly (L-lactic acid) nanocomposite scaffold. Biomater. 2003; 24(16): 2773-2778.

10. Samadian H, Salehi M, Farzamfar S, Vaez A, Ehterami A, Sahrapeyma H, Goodarzi A, Ghorbani S. In vitro and in vivo evaluation of electrospun cellulose acetate/gelatin/ hydroxyapatite nanocomposite mats for wound dressing applications. Artif Cells Nanomed Biotechnol. 2018; 46(sup1): 964-974.

11. Kumta PN, Sfeir C, Lee D-H, Olton D, Choi D. Nanostructured calcium phosphates for biomedical applications: novel synthesis and characterization. Acta Biomater. 2005; 1(1): 65-83.

12. Matsumoto T, Okazaki M, Inoue M, Yamaguchi S, Kusunose T, Toyonaga T, Hamada Y, Takahashi J. Hydroxyapatite particles as a controlled release carrier of protein. Biomater. 2004; 25(17): 3807-3812.

13. Mizushima Y, Ikoma T, Tanaka J, Hoshi K, Ishihara T, Ogawa Y, Ueno A. Injectable porous hydroxyapatite microparticles as a new carrier for protein and lipophilic drugs. J Control Release. 2006; 110(2): 260-265.

14. Tamm T, Peld M. Computational study of cation substitutions in apatites. J Solid State Chem. 2006; 179(5): 1581-1587.

15. P Busardo F, Frati P, Di Sanzo M, Napoletano S, Pinchi E, Zaami S, Fineschi V. The impact of nandrolone decanoate on the central nervous system. Curr Neuropharmacol. 2015; 13(1):122-131.

16. Pardridge WM. 4 Serum bioavailability of sex steroid hormones. Best Pract Res Clin Endocrinol Metab. 1986; 15(2): 259-278.

17. Riezzo I, Turillazzi E, Bello S, Cantatore S, Cerretani D, Di Paolo M, Fiaschi AI, Frati P, Neri M, Pedretti M. Chronic nandrolone administration promotes oxidative stress, induction of pro-inflammatory cytokine and TNF-α mediated apoptosis in the kidneys of CD1 treated mice. Toxicol Appl Pharmacol. 2014; 280(1): 97-106.

18. Bahrke MS, Yesalis CE, Wright JE. Psychological and behavioural effects of endogenous testosterone and anabolic-androgenic steroids. Sports Med. 1996; 22(6): 367-390.

19. Buckley WE, Yesalis CE, Friedl KE, Anderson WA, Streit AL, Wright JE. Estimated prevalence of anabolic steroid use among male high school seniors. Jama. 1988; 260(23): 3441-3445.

20. Durant RH, Rickert VI, Ashworth CS, Newman C, Slavens G. Use of multiple drugs among adolescents who use anabolic steroids. N Engl J Med Overseas Ed 1993;328(13):922-926.

21. Kopera H. The history of anabolic steroids and a review of clinical experience with anabolic steroids. Acta Endocrinol. 1985; 110(3 Suppla): S11-S18.

22. Eklöf A-C, Thurelius A-M, Garle M, Rane A, Sjöqvist F. The anti-doping hot-line, a means to capture the abuse of doping agents in the Swedish society and a new service function in clinical pharmacology. Eur J Clin Pharmacol. 2003; 59(8-9): 571-577.

23. Verroken M. Ethical aspects and the prevalence of hormone abuse in sport. J Endocrinol. 2001; 170(1): 49-54.

24. Sun L, Pan J, Peng Y, Wu Y, Li J, Liu X, Qin Y, Bauman WA, Cardozo C, Zaidi M. Anabolic steroids reduce spinal cord injury-related bone loss in rats associated with increased Wnt signaling. J Spinal Cord Med. 2013; 36(6): 616-622.

25. Ahmad F, Yunus SM, Asghar A, Faruqi N. Influence of anabolic steroid on tibial fracture healing in rabbits–a study on experimental model. J Clin Diagn Res. 2013; 7(1): 93.

26. Salehi M, Naseri-Nosar M, Ebrahimi-Barough S, Nourani M, Vaez A, Farzamfar S, Ai J. Regeneration of sciatic nerve crush injury by a hydroxyapatite nanoparticle-containing collagen type I hydrogel. Jpn J Physiol. 2018; 68(5): 579-587.

27. Tanaka K, Shiga T, Katayama T. Fabrication of hydroxyapatite/ PLA composite nanofiber by electrospinning. High Performance and Optimum Design of Structures and Materials II. 2016; 166: 371.

28. Shahrezaee M, Salehi M, Keshtkari S, Oryan A, Kamali A, Shekarchi B. In vitro and in vivo investigation of PLA/PCL scaffold coated with metformin-loaded gelatin nanocarriers in regeneration of critical-sized bone defects. Nanomed. 2018; 14(7): 2061-2073.

29. Hannink G, Arts JC. Bioresorbability, porosity and mechanical strength of bone substitutes: what is optimal for bone regeneration? Inj. 2011; 42: S22-S25.

30. Karp JM, Shoichet MS, Davies JE. Bone formation on two-dimensional poly (DL-lactide-co-glycolide)(PLGA) films and three-dimensional PLGA tissue engineering scaffolds in vitro. J Biomed Mater Res A. 2003; 64(2): 388-396.

31. Bose S, Roy M, Bandyopadhyay A. Recent advances in bone tissue engineering scaffolds. Trends Biotechnol. 2012; 30(10): 546-554.

32. Bat E, Zhang Z, Feijen J, Grijpma DW, Poot AA. Biodegradable elastomers for biomedical applications and regenerative medicine. Regen Med. 2014; 9(3): 385-398.

33. Abbasian M, Massoumi B, Mohammad-Rezaei R, Samadian H, Jaymand M. Scaffolding polymeric biomaterials: Are naturally occurring biological macromolecules more appropriate for tissue engineering? Int J Biol Macromol. 2019.

34. Liao S, Cui F, Zhang W, Feng Q. Hierarchically biomimetic bone scaffold materials: nano-HA/collagen/PLA composite. J Biomed Mater Res B. 2004; 69(2): 158-165.

35. Yoshikawa H, Myoui A. Bone tissue engineering with porous hydroxyapatite ceramics. Art Org. 2005; 8(3): 131-136.

36. Akindoyo JO, Beg MD, Ghazali S, Heim HP, Feldmann M. Effects of surface modification on dispersion, mechanical, thermal and dynamic mechanical properties of injection

122

Nanomed. J. 7(2): 115-123, Spring 2020

molded PLA-hydroxyapatite composites. Compos A. 2017; 103: 96-105.

37. Wu C, Ramaswamy Y, Zhu Y, Zheng R, Appleyard R, Howard A, Zreiqat H. The effect of mesoporous bioactive glass on the physiochemical, biological and drug-release properties of poly (DL-lactide-co-glycolide) films. Biomater. 2009; 30(12): 2199-2208.

38. Yuan J, Shen J, Kang IK. Fabrication of protein-doped PLA composite nanofibrous scaffolds for tissue engineering. Polym Int. 2008; 57(10):1188-1193.

39. Fratzl P, Gupta H, Paschalis E, Roschger P. Structure and mechanical quality of the collagen–mineral nano-composite in bone. J Mater Chem. 2004; 14(14): 2115-2123.

40. Yuan H, Li Y, De Bruijn J, De Groot K, Zhang X. Tissue responses of calcium phosphate cement: a study in dogs. Biomater. 2000; 21(12): 1283-1290.

41. Kilpadi KL, Chang PL, Bellis SL. Hydroxylapatite binds more serum proteins, purified integrins, and osteoblast precursor cells than titanium or steel. J Biomed Mater Res A. 2001; 57(2): 258-267.

42. Karageorgiou V, Kaplan D. Porosity of 3D biomaterial scaffolds and osteogenesis. Biomater. 2005; 26(27): 5474-5491.

43. Boccaccio A, Uva AE, Fiorentino M, Bevilacqua V, Pappalettere C, Monno G. A Computational Approach to the Design of Scaffolds for Bone Tissue Engineering. Adv Biomater. 2018. p. 111-117.

44. Murphy CM, Haugh MG, O'Brien FJ. The effect of mean pore size on cell attachment, proliferation and migration in collagen–glycosaminoglycan scaffolds for bone tissue engineering. Biomater. 2010; 31(3): 461-466.

45. Ramesh N, Moratti SC, Dias GJ. Hydroxyapatite–polymer biocomposites for bone regeneration: A review of current trends. J Biomed Mater Res B. 2018; 106(5): 2046-2057.

46. Huyck L, Ampe C, Van Troys M. The XTT cell proliferation assay applied to cell layers embedded in three-dimensional matrix. Assay Drug Dev Technol. 2012; 10(4): 382-392.

47. Zeng Q, Hong W. The emerging role of the hippo pathway in cell contact inhibition, organ size control, and cancer development in mammals. Cancer cell. 2008; 13(3): 188-192.

48. Vannucci L, Brandi ML. Healing of the bone with anti-fracture drugs. Expert Opin Pharmacother. 2016; 17(17): 2267-2272.

49. Demling RH. Oxandrolone, an anabolic steroid, enhances the healing of a cutaneous wound in the rat. Wound Repair Regen. 2000; 8(2): 97-102.

50. Guimarães APFGM, Butezloff MM, Zamarioli A, Issa JPM, Volpon JB. Nandrolone decanoate appears to increase bone callus formation in young adult rats after a complete femoral fracture. Acta Cir Bras. 2017; 32(11): 924-934.

51. Ogasawara A, Nakajima A, Nakajima F, Goto K-i, Yamazaki M. Molecular basis for affected cartilage formation and bone union in fracture healing of the streptozotocin-induced diabetic rat. Bone. 2008; 43(5): 832-839.

52. Urabe K, Kim HJ, Sarkar G, Bronk JT, Bolander ME. Determination of the complete cDNA sequence of rat type II collagen and evaluation of distinct expression patterns of types IIA and IIB procollagen mRNAs during fracture repair in rats. Ortho Sci. 2003; 8(4): 585-590.

53. Pansieri JC, Esteves A, Junior WCR. Anabolic Steroids Effects on Bone Regeneration. Sport Sci. 2019; 7(3): 88-93.

Nanomed. J. 7(2): 115-123, Spring 2020

123